

MACHINE IMPEDANCE CALCULATION AND OPTIMIZATION OF VACUUM COMPONENTS IN SLS 2.0

A. Citterio, J. P. Braschoss IV, M. Dehler, S. Dordevic, D. Stephan, L. Stingelin,
Paul Scherrer Institut, 5232 Villigen PSI, Switzerland

Abstract

For a reliable determination of the single bunch stability threshold, the broadband impedance budget needs to be analysed for all resistive and inductive contributions. The completely new design of the arc vacuum chamber of SLS 2.0 with respect to SLS [1] - now with a reduced beam pipe diameter, and coated with layers of copper and NEG - requires special focus on the resistive wall impedance.

Higher Order Modes (HOMs) of vacuum components were also investigated. Since they stay trapped in specific positions of the ring, they can be the source of power heating and related mechanical stress, as well as the cause of Coupled Bunch Instabilities (CBI). The impact of the HOM impedance spectrum can become very important, notably if the device responsible of the resonance recurs several times in the ring or if it is located at positions with high beta values. We show some examples of HOM analysis and their related optimization, which were adopted for cavities appearing also in valves, bellows and diagnostic components.

BROADBAND IMPEDANCE BUDGET

The resistive wall represents a major contribution to the broadband impedance budget which is used for the determination of the single bunch instability thresholds of SLS 2.0. The cross section of the arc vacuum chamber has an octagonal shape, with 18 mm distance between opposite faces and a 3 mm opening slit between the electron channel and the antechamber. In the straight sections, where RF cavities and undulators are installed, the cross section of the vacuum chamber is round, with diameters suitable for the different components located there. Compared to the current design of the SLS ring, mainly in stainless steel and aluminium and with a 32 mm vertical gap, the 18 mm aperture of SLS 2.0 causes higher resistive wake-field effects, partially compensated by copper material. The Non Evaporable Getter (NEG) coating, applied for better vacuum pumping and desorption, has a nominal thickness of 500 nm in order to avoid a major increase of the resistive wall impedance. The injection straight design is characterized by metallised ceramic, stainless steel and copper chambers, with a wide variation in the vertical beam aperture, from a minimum of 11 mm (thin septum) to 40 mm maximum (injection kickers). Finally, the cross sections of the Insertion Devices (IDs) include round, elliptical and rectangular shapes, with vertical gaps varying from 3.5 to 9 mm according to the beamlines.

The full SLS 2.0 resistive wall impedance of SLS 2.0 was computed with the code ImpedanceWake2D [2]. With

good approximation, the 18 mm octagon chamber is modelled with a circular chamber of the same diameter. The copper conductivity is set equal to $5.7 \cdot 10^7$ S/m, while the NEG conductivity is of the dense type - $\sigma_{NEG} = 8 \cdot 10^5$ S/m - as validated by the measurement campaign described in [3,4]. Table 1 shows the resistive wall loss factors over the whole 288 meters synchrotron circumference with all the IDs installed, calculated for Gaussian single bunches of 3, 6 and 9 mm rms.

Table 1: Resistive Wall Loss Factors (The IDs are at Minimum Gap).

RW	k [V/pC] ($\sigma_b = 3$ mm)	k [V/pC] ($\sigma_b = 6$ mm)	k [V/pC] ($\sigma_b = 9$ mm)
Vacuum chamber	3.0	1.1	0.6
IDs	1.4	0.5	0.3

In Table 1, the 3 mm bunch length is typical of the beam operation without harmonic cavity, while with the harmonic cavity the bunch lengths are between 6 and 9 mm RMS [5].

In the initial part of the resistive wall spectrum - few tenth of GHz -, the inductance L_{RW} is in a first approximation constant with the frequency, and equal to 5.3 nH. This amount is increased by the effect of the average surface roughness of the beam pipe chamber, specified as 0.6 μ m RMS for the milling technique. Semi-analytical calculations, based on the wake-field model in a waveguide coated with thin dielectric layer [6], allowed to estimate the roughness contribution to about 2 nH for the full ring. Then, the resistive wall together with the roughness are responsible for a total inductance of 7.3 nH.

The aperture of the vacuum chamber is, together with the magnet configuration in the lattice, one important parameter defining the Coherent Synchrotron Radiation (CSR) in the longitudinal short range wake-fields. For SLS 2.0, the CSR is modelled looking to the approximation of infinite parallel plate, steady state regime of a bend [7], with a vertical gap of 18 mm. On that conservative approximation, the CSR impedance produced by each magnet slice is linearly added one to each other, in order to obtain the global contribution. Mainly because of the shielding provided by the vacuum chamber, and for the choice of a positive momentum compaction factor, the CSR remains negligible inside the bunch spectra with respect to all the other impedance components.

The contribution to the geometrical short range wake fields, simulated with ABCI [8] and CST Studio Suite [9], takes into account cavities, such as the four 500 MHz RF cavities, the superconducting 3rd harmonic cavity, Beam

Positions Monitors (BPMs), kickers, vacuum components like bellows and valves and several kind of tapers. With respect to the tapers, a maximum angle of 100 mrad was decided as general upper limit, to guarantee smooth enough transitions between the cross sections of the chamber. It is also worth to mention that the BPMs have a special off-centre design of the RF feedthroughs [1] in order to ensure HOM suppression and negligible heating. As for the resistive wall, the most relevant loss factors coming from the geometrical short range wakes are listed in Table 2, again for three typical Gaussian bunches.

Table 2: Geometrical Loss Factors.

Devices	k [V/pC] ($\sigma_b = 3$ mm)	k [V/pC] ($\sigma_b = 6$ mm)	k [V/pC] ($\sigma_b = 9$ mm)
127 BPMs	2.7	0.4	0.1
500 MHz cavities	5.2	3.7	3.0
Super-3HC (2 cells)	1.8	0.9	0.6
Transverse kickers	3.5	2.2	1.5
Longitudinal kicker	1.7	1.3	1.0
Fast injection kickers	1.3	0.4	0.3
Bellows, valves	0.9	0.2	0.2

The total longitudinal and transverse broadband impedance spectra are shown in Fig. 1 and 2 respectively.

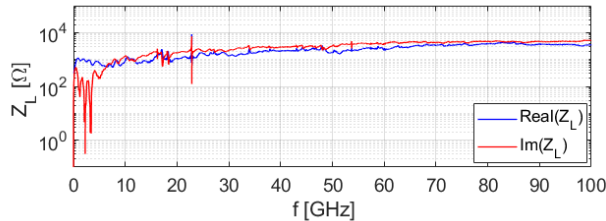


Figure 1: Frequency spectrum of the real and imaginary part of the longitudinal broadband impedance.

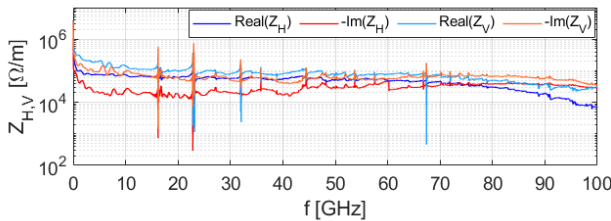


Figure 2: Frequency spectrum of the real and imaginary part of the horizontal and vertical broadband impedances, scaled for the normalized beta functions.

Most of the components, which are included for the present broadband impedance budget in Fig. 1 and 2, are at the final design stage, and only a minor part, located especially

in the injection straight, is still under optimization process, e.g. the thin septum. A few changes in the broadband impedance are then expected, without significant discrepancies in the estimation of the instability thresholds.

EXAMPLES OF HIGHER ORDER MODES IN VACUUM COMPONENTS

We present here two examples of vacuum components, where a special RF design is needed to keep the potential trapped HOMs inside the safety margins of the coupled bunch instabilities [5], avoiding at the same time possible heating issues. These components are the 21 mm diameter bellow and valve assembly, and the collimators installed at the two long straights of SLS 2.0. The analysis of the HOMs profited from both wake-field and eigenmode simulations performed with CST Studio Suite.

Sector Bellows and Valves

At every beginning and end of the 12 straights of SLS 2.0, one bellow and one valve of 21 mm diameter will be installed. Taking into account also some additional locations in the ring, a total amount of about 30 bellows and valves of this kind are foreseen [10]. These vacuum components, developed and supplied by VAT Group AG [11], are based on one optimized design, which keeps the HOM spectrum well within the stability thresholds and the mechanical specs.

The bellow chamber seen by the beam is composed of a central RF shielding in stainless steel coated with a silver layer, and two sleeves in stainless steel. The DC continuity are ensured by multiple contact points on each sleeve. The maxima longitudinal and transverse displacements are specified in ± 6 mm and ± 1.5 mm respectively. The valve has a comb design and a flexible RF shielding is placed behind the interleaved rigid fingers and the connected sleeve. The material chosen for both the comb and the sleeve is uncoated stainless steel. The interface between the bellow and valve is realized by a “spring-loaded” flange, which guarantees zero gap in between the two devices. Figure 3 shows the assembly, and Table 3 gives, for one fixed geometry configuration, the summary of the two main longitudinal HOMs, trapped below the beam pipe cut-off.

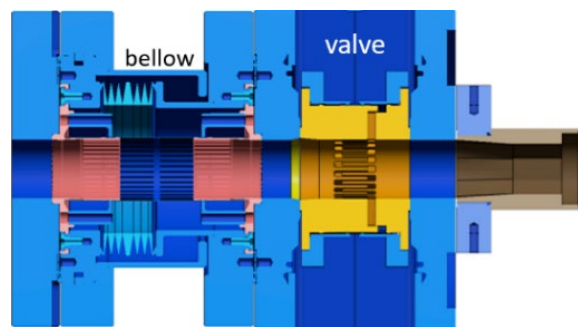


Figure 3: DN21 bellow (left) and valve (right) assembly (only a part of the body valve is shown here).

Table 3: Impedance Parameters for The Longitudinal Homs Trapped in the Bellow and Valve Assembly. The Values are for a Bunch Length Of 3 Mm RMS (no harmonic cavity).

Location	f [GHz]	Q	R/Q [Ω]	P_{max} [W]	$30 \cdot Rf$ [$k\Omega$ GHz]
Valve	1.271	65	1.40	28	3.4
Valve, bellow	10.861	339	0.04	2.7	2.8

Because in SLS 2.0 the minimum longitudinal coupled bunch instability threshold is set to 25 $k\Omega$ GHz [5], no excitation raises from these longitudinal HOMs. The lowest HOM in the spectrum is fully located in the comb volume of the valve, and it gives the largest dissipated power P_{max} , calculated at 400 mA beam current and with the resonance tuned to the closest RF harmonic. That power is mainly distributed to the sleeve (16 Watt), and to the two comb (9.5 Watt). The second mode still originates in the valve, where most of its power is dissipated, and it leaks weakly into the bellow. Thermal simulations tested the mechanical stress of the different pieces in the assembly show enough safety margin concerning the heating of the different components. In the transverse planes, only one HOM is trapped in the valve at 1.496 GHz. Assuming the same impedance from each valve, a total transverse impedance of 1.4 $M\Omega/m$ is obtained: this amount is well below the threshold of the transverse coupled bunch instabilities [5].

Collimators

One pair of horizontal and vertical collimators is installed at each of the two long straights of SLS 2.0, where the quadrupole triplets are located: after the 500 MHz RF cavities in straight 5, and after the Super-3HC in straight 9. At these locations, the horizontal and vertical beta functions can reach very large values [1]. Figure 4 shows the schematic volume used for the impedance calculations.

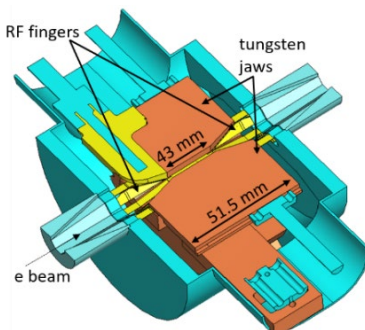


Figure 4: Top view of the collimator.

The goal of the two movable tungsten jaws seen in Fig. 4 consists in capturing the halo-particles, localizing the losses and preventing the radiation damages to critical devices, such as the cooled in-vacuum undulators. The minimum aperture the collimator chamber can achieve is 7.2 mm, while 8 mm will be more often used during beam operations. The jaw taper angle measures 16.5°.

Trapped HOMs are here efficiently avoided by copper beryllium (CuBe) RF fingers – ten at the entrance and ten at the exit of the collimator - which guarantee the electrical contacts between the internal tapered chamber and the external volume. Also, the beam pipe transition to the collimator was carefully designed to minimize the overall impedance.

The present design fulfils the impedance specifications, for both the apertures of 7.2 and 8 mm. In the longitudinal plane, the impedance contribution is mainly inductive, with negligible residual resonances: at the configuration with minimum gap, a maximum of 16 Watt is dissipated in the whole collimator, with 1.3 Watt distributed in each of the two CuBe finger foils. In the two transverse planes, the eigenmode analysis of the HOMs still trapped in the cavity does not present issues in terms of coupled bunch instabilities: the collimator thresholds, set at 3.7 and 2.3 $M\Omega/m$ for the horizontal and vertical plane respectively [5], are well above the transverse impedance calculated. The transverse impedance is summarized in Fig. 5, for a geometry with the minimum aperture width of 7.2 mm, and without resistive losses.

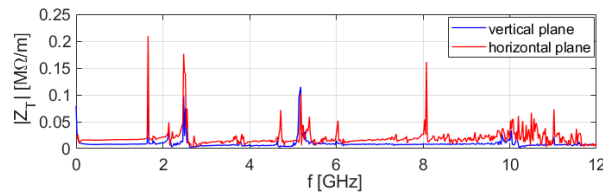


Figure 5: Transverse impedance spectra (magnitude) of one horizontally tapered collimator.

CONCLUSION

The main aspects of the broadband impedance spectra in SLS 2.0 were summarized, focusing on the major resistive and inductive contributions. The impedance budget is very close to be completed, and it can be used to determine the single bunch instability thresholds [5].

Two examples of HOM investigation in vacuum components - sector bellow/valve assembly, collimators – show the important benefits of one optimized design, both in terms of power heating and CBI suppression. Additional RF devices (kickers) optimized for the HOMs in SLS 2.0 are described in [12].

ACKNOWLEDGEMENTS

The design of the bellows and valves which will be installed in SLS 2.0 was done in a tight working relationship with VAT Company: the optimization of the RF and engineering aspects of these devices greatly profited from the experience and the innovative solutions VAT presented for SLS 2.0.

For the collimator design we benefited strongly from advice and support of S. White and T. Brochard (ESRF).

REFERENCES

[1] “SLS 2.0 Storage Ring Technical Design Report”, PSI Bericht, Villigen PSI, Switzerland, Rep. 21-02, Nov. 2021.

[2] ImpedanceWake2D,
<https://twiki.cern.ch/twiki/bin/view/ABPComputing/ImpedanceWake2D>

[3] M. Dehler *et al.*, “Characterization of NEG Coatings for SLS 2.0”, in *Proc. IPAC’19*, Melbourne, Australia, May 2019, pp. 1662-1665.
doi:10.18429/JACoW-IPAC2019-TUPGW108

[4] M. Dehler *et al.*, “RF Characterization of Thin NEG Coatings in the Sub THz Range”, in *Proc. MULCOPIM’22*, Oct. 2022, Valencia, Spain.

[5] A. Citterio, M. Dehler, L. Stingelin, “Overview on the collective effects in SLS 2.0”, presented at IPAC’23, Venice, Italy, May 2023, paper MOPM017.

[6] A. Novokhatski, M. Timm and T. Weiland, “The Surface Roughness Wakefield Effect”, in *Proc. ICAP’98*, Monterey, CA, USA, Sep. 1998.

[7] R. L. Warnock, SLAC-PUB-5379 November (1990).

[8] Y.H. Chin, “User’s Guide for ABCI Version 9.4 and Introducing the ABCI Windows Application Package,” KEK Report (2005) 2005-06.

[9] CST Studio Suite, <https://www.3ds.com/products-services/simulia/products/cst-studio-suite/>.

[10] R. Ganter *et al.*, “SLS 2.0 Storage Ring Components overview before installation”, Presented at IPAC’23, Venice, Italy, May 2023, paper MOPM020.

[11] VAT Group AG, <https://www.vatvalve.com/>.

[12] M. Dehler *et al.*, “Fast kickers for bunch by bunch feedbacks at SLS 2.0 and ELETTRA 2.0”, IPAC2023, Venice, Italy, May 2023, paper THPL149.